

UCLA

UCLA Previously Published Works

Title

MAFG Is a Transcriptional Repressor of Bile Acid Synthesis and Metabolism

Permalink

<https://escholarship.org/uc/item/7528f722>

Journal

Cell Metabolism, 21(2)

ISSN

1550-4131

Authors

de Aguiar Vallim, Thomas Q
Tarling, Elizabeth J
Ahn, Hannah
[et al.](#)

Publication Date

2015-02-01

DOI

10.1016/j.cmet.2015.01.007

Peer reviewed

Published in final edited form as:

Cell Metab. 2015 February 3; 21(2): 298–310. doi:10.1016/j.cmet.2015.01.007.

MAFG Is a Transcriptional Repressor of Bile Acid Synthesis and Metabolism

Thomas Q. de Aguiar Vallim^{1,8}, Elizabeth J. Tarling¹, Hannah Ahn¹, Lee R. Hagey², Casey E. Romanoski³, Richard G. Lee⁴, Mark J. Graham⁴, Hozumi Motohashi⁵, Masayuki Yamamoto⁶, and Peter A. Edwards^{1,7,8}

¹Division of Cardiology, David Geffen School of Medicine, University of California, Los Angeles, California, USA

²Department of Medicine, University of California, San Diego, La Jolla, California, USA

³Department of Cellular and Molecular Medicine, University of California, San Diego, La Jolla, California, USA

⁴ISIS Pharmaceuticals, Carlsbad, CA 92010, USA

⁵Department of Gene Expression Regulation, Institute of Development, Aging and Cancer, Sendai, Japan

⁶Department of Medical Biochemistry, Tohoku Medical Megabank Organization, Sendai, Japan

⁷Department of Biological Chemistry, University of California, Los Angeles, California, USA

Summary

Specific bile acids are potent signaling molecules that modulate metabolic pathways affecting lipid, glucose and bile acid homeostasis and the microbiota. Bile acids are synthesized from cholesterol in the liver, and the key enzymes involved in bile acid synthesis (*Cyp7a1*, *Cyp8b1*) are regulated transcriptionally by the nuclear receptor FXR. We have identified an FXR-regulated pathway upstream of a transcriptional repressor that controls multiple bile acid metabolism genes. We identify *MafG* as an FXR target gene and show that hepatic MAFG overexpression represses genes of the bile acid synthetic pathway, and modifies the biliary bile acid composition. In contrast, loss-of-function studies using *MafG*^{+/-} mice causes de-repression of the same genes with

© 2015 Elsevier Inc. All rights reserved.

⁸Correspondence should be addressed to P.A.E. (pedwards@mednet.ucla.edu) and T.Q. de A.V. (tvallim@mednet.ucla.edu).

Publisher's Disclaimer: This is a PDF file of an unedited manuscript that has been accepted for publication. As a service to our customers we are providing this early version of the manuscript. The manuscript will undergo copyediting, typesetting, and review of the resulting proof before it is published in its final citable form. Please note that during the production process errors may be discovered which could affect the content, and all legal disclaimers that apply to the journal pertain.

Supplemental Information. Supplemental Information includes Extended Experimental Procedures, six figures and two tables.

Author Contributions

T.Q. de A.V. and P.A.E. conceived the project and wrote the manuscript. L.R.H. carried out bile acid analysis, H.M. and M.Y. provided *MafG*^{+/-} mice and R.L. and M.G. provided the MafG ASO. C.R. carried out ChIP-Seq bioinformatics analysis. All authors provided feedback during preparation of the manuscript. T.Q. de A.V. executed all experiments, and was aided by H.A., and E.J.T.

Competing Financial Interests

R. Lee and M. Graham are employees and shareholders of Isis Pharmaceuticals. All other authors have no financial interests to disclose.

concordant changes in biliary bile acid levels. Finally, we identify functional MafG response elements in bile acid metabolism genes using ChIP-Seq analysis. Our studies identify a molecular mechanism for the complex feedback regulation of bile acid synthesis controlled by FXR.

Introduction

Bile acids function both as detergents that facilitate lipid absorption, and as endogenous ligands that regulate metabolic pathways through activation of several nuclear receptors, including the Farnesoid-X-Receptor (FXR, Nr1h4) as well as TGR5, a G-protein-coupled receptor (de Aguiar Vallim et al., 2013a). Although FXR plays a particularly important role in maintaining bile acid homeostasis, numerous studies have shown that FXR directly regulates many genes that affect multiple metabolic cascades (de Aguiar Vallim et al., 2013a; Evans and Mangelsdorf, 2014). Consistent with these findings, mice lacking FXR exhibit not only dysregulated bile acid metabolism, but also abnormal lipoprotein (Sinal et al., 2000) and glucose metabolism (Duran-Sandoval et al., 2005; Zhang et al., 2006), increased hepatic susceptibility to certain toxins (Lee et al., 2010), increased levels of ileal bacteria and impaired barrier function of intestinal epithelia (Inagaki et al., 2006). Reduced FXR signaling is also associated with obesity, possibly as a result of bile acid-dependent modulation of the microbiota (Li et al., 2013; Ridaura et al., 2013). Moreover, a recent study demonstrated that in mice, the benefits of bariatric surgery may be mediated by FXR signaling to modulate bile acid-dependent effects on the microbiota (Ryan et al., 2014). Thus, the findings that elevated bile acid levels in humans and/or mice are associated with gastro-intestinal diseases, hepatotoxicity, altered plasma lipoprotein levels and aberrant glucose metabolism suggest that abnormal control of the bile acid pool can have broad physiological effects (de Aguiar Vallim et al., 2013a; Kuipers et al., 2014).

Although negative feedback of bile acid synthesis was first described over 50 years ago (Beher et al., 1961), the precise mechanisms by which bile acids mediate this repression are still not fully understood. The enzymatic catabolism of cholesterol, or hydroxysterols, to form primary bile acids occurs via either the classic or alternative pathways (Fig. 1A). These two pathways generate approximately 75% and 25% respectively, of the total primary bile acids and involve at least 17 enzymes (Russell, 2003) (Fig. 1A). Within the classic pathway, CYP7A1 is the rate-limiting enzyme while CYP8B1 regulates the synthesis of cholic acid (Li-Hawkins et al., 2002) and thus regulates the bile acid pool composition (Fig. 1A). The transcription of both *Cyp7a1* and *Cyp8b1* are particularly responsive to end product feedback control (Russell, 2003). In contrast, the alternative bile acid pathway involves CYP7B1 and CYP27A1 (Fig. 1A) (Russell, 2003). Little is known about the regulation of the genes that encode enzymes of the alternative pathway, or downstream of CYP7A1 and CYP8B1. Nonetheless, the findings that a number of diseases result from mutations of *CYP7A1*, *CYP7B1*, *CYP27A1*, *HSD3B7*, *AMACR* or *AKR1C4* (*Akr1c14* in mice) (Fig. 1A), emphasizes the importance of maintaining normal bile acid synthesis and homeostasis.

In humans and mice, one of the most abundant bile acids is cholic acid (CA). Humans also have high levels of chenodeoxycholic acid (CDCA). In contrast, mice almost quantitatively convert CDCA to muricholic acid (MCA) (Fig. 1 A) (de Aguiar Vallim et al., 2013a;

Russell, 2003). The negative feedback regulation of bile acid synthesis is largely dependent on activation of hepatic and/or intestinal FXR (Kim et al., 2007). Such activation results in induction of small heterodimerizing partner (*Shp*, *Nr0b2*) in the liver (Kerr et al., 2002; Wang et al., 2002), and *Fgf15* (mouse) or *FGF19* (human) in the small intestine (Inagaki et al., 2005; Inagaki et al., 2006). SHP does not bind DNA directly but rather binds to other transcription factors such as HNF4 α and LRH-1 to impair their function (Bavner et al., 2005; Goodwin et al., 2000; Lu et al., 2000). In contrast, intestinally-derived FGF15/19 is secreted into the blood before binding to the FGFR4/ β -Klotho receptor on the surface of hepatocytes to initiate an incompletely understood pathway which leads to repression of *Cyp7a1* (Inagaki et al., 2005). In contrast to the detailed studies detailing the mechanisms that control *Cyp7a1*, the mechanisms involved in the repression of *Cyp8b1*, and thus cholic acid synthesis, are less well understood. Nonetheless, FXR activation is known to repress *Cyp8b1* expression by mechanisms that may also involve SHP and FGF15/19 (Kerr et al., 2002; Kong et al., 2012; Wang et al., 2002).

Here, we identify a previously unrecognized FXR-regulated pathway involving MAFG (V-Maf Avian Musculoaponeurotic Fibrosarcoma Oncogene Homolog G), a member of the MAF family of transcription factors. We show that *MafG* is a direct target gene of FXR and hepatic overexpression of MAFG in mice represses genes encoding enzymes of the classic and alternative pathways. In addition, overexpression of MAFG in mice resulted in a decrease in biliary cholic acid levels and an increase in muricholic acid levels, a finding consistent with the greater inhibition of *Cyp8b1* as compared to *Cyp7a1*. Finally, we utilize loss-of-function approaches (knockdown of *MafG* with antisense oligonucleotides, *MafG*^{+/-} mice) to show that a 50–80% loss of hepatic MAFG protein results both in de-repression of many of the same genes, including *Cyp8b1*, and an increase in biliary cholic acid levels. In conclusion, our results identify an FXR-*MafG* pathway that functions in the feedback repression of bile acid metabolism by modulating the composition of the bile acid pool.

Results

FXR Activation Represses both the Classic and Alternative Bile Acid Synthetic Pathways

Multiple studies have shown that activated FXR leads to repressed transcription of both *Cyp7a1* and *Cyp8b1* (Kerr et al., 2002; Kong et al., 2012; Wang et al., 2002). While the mechanisms regulating *Cyp7a1* expression have been extensively studied, much less is known about how FXR represses *Cyp8b1* or whether FXR regulates the expression of other genes involved in the two bile acid synthetic pathways. In our initial studies we treated wild-type and *Fxr*^{-/-} mice (KO) for 3 days with either GW4064, a widely used FXR agonist (Maloney et al., 2000), or GSK2324 a water-soluble derivative of GW4064 that exhibits increased potency (Bass et al., 2011). As expected, both agonists led to robust repression of both *Cyp7a1* and *Cyp8b1* in wild-type, but not *Fxr*^{-/-} mice (Fig. 1B). Importantly, both agonists also resulted in an FXR-dependent repression of *Cyp7b1* and *Cyp27a1* in the alternative pathway (Fig. 1C). In addition, we measured the hepatic mRNA levels of a number of additional genes that encoded enzymes involved in bile acid synthesis. We now show for the first time that FXR activation in wild-type but not *Fxr*^{-/-} mice results in repression of numerous bile acid synthetic genes, including *Acox2*, *Akr1c14*, *Hsd3b7*,

Hsd17b4, *Scp2* and *Slc27a5* (Fig. 1D). In contrast, *Amacr* and *Cyp39a1* mRNA levels are unchanged (Fig. 1D) while *Akr1d1* is modestly induced after FXR activation, consistent with ChIP-Seq data that identifies a putative intronic FXRE in the *Akr1d1* locus (Fig. S1A). Overall, the repression of most bile acid synthetic genes was not as pronounced as that observed for *Cyp8b1* and *Cyp7a1* (Fig. 1B). Nevertheless, these studies demonstrate that treatment of mice with two different synthetic FXR agonists results in repression of genes involved in both the classic and alternative bile acid synthetic pathways, consistent with a central role for FXR in regulating all aspects of bile acid synthesis.

FXR Activation Induces the Expression of Several Transcriptional Repressors

The nuclear receptor FXR binds to its cognate response element (FXRE) as an FXR:RXR heterodimer and functions almost exclusively as a transcriptional activator (de Aguiar Vallim et al., 2013a). Nonetheless, although activation of FXR leads to induction of many hepatic genes, it also results in repression of numerous genes involved in bile acid metabolism (Fig. 1D). A number of studies have demonstrated that the mechanisms involved in the repression of *Cyp7a1*, *Cyp8b1* are indirect and are the result of the FXR-dependent increased expression of *Shp* and *Fgf15/19* that encode proteins that function to inhibit transcription of specific genes (de Aguiar Vallim et al., 2013a; Kuipers et al., 2014). One additional mechanism by which FXR causes a reduction in specific genes is through miRNAs. For example, we recently identified miR-144 as an FXR-regulated miRNA that subsequently targets ABCA1 (de Aguiar Vallim et al., 2013b). Based on these earlier studies we hypothesized that FXR activation might increase the expression of additional repressors that function to control metabolic pathways.

To identify such putative transcriptional repressors, we re-analyzed the data from our prior ChIP-Seq study that had been used to identify global hepatic FXR response elements (FXREs) (Chong et al., 2010). Gene ontology analysis identified a significant enrichment in transcription factors containing FXREs (Chong et al., 2010). Consequently, we searched this subset of FXRE-containing genes, focusing specifically on genes annotated to have transcriptional repressor activity. Our analysis identified four putative transcriptional repressor genes, namely *Shp*, a well-characterized FXR target gene, v-maf musculoaponeurotic fibrosarcoma oncogene homolog G (avian) (*MafG*), cysteine-rich intestinal protein 2 (*Crip2*) and Zinc-finger protein 385a (*Zfp385a*). We also identified a fifth putative transcriptional repressor, Oligodendrocyte transcription factor 1 (*Olig1*), which we show can be regulated by FXR agonists (Fig. S1B) and contains an FXRE in its genomic loci. However, since the hepatic expression of *Olig1* is very low (data not shown), we have not studied this gene further.

To confirm the presence of FXREs at the loci of these putative transcriptional repressors, we analyzed a second independent FXR ChIP-Seq data set from mouse livers (Thomas et al., 2010). This analysis verified that *Crip2* (Fig. 2A), *MafG* (Fig. 2B), *Zfp385a* (Fig. 2C), and *Shp* (Fig. S1C) contained one or more FXREs at their genomic loci. To investigate whether these genes were regulated in response to FXR and FXR agonists, we measured the hepatic expression of *Crip2*, *MafG* and *Zfp385a* in wild-type and *Fxr*^{-/-} mice (KO) pre-treated for 3 days with either GW4064 or GSK2324. We utilized a dose of 60mpk/day to directly

compare the effects of the two agonists. In all experiments, *Shp* and/or *Bsep*, both well characterized FXR-target genes (Ananthanarayanan et al., 2001; Goodwin et al., 2000), served as positive controls. Hepatic *MafG*, *Crip2*, *Zfp385a* and *Shp* mRNA levels were all significantly induced following treatment of wild-type mice, but not *Fxr*^{-/-} mice (KO), with either FXR agonist (Fig. 2D), demonstrating that induction was FXR-dependent. Further, induction of each gene was greater after treatment with GSK2324 as compared to GW4064 (Fig. 2D), consistent with increased potency of GSK2324. In the case of MAFG, the levels of protein were induced 2–3 fold following treatment of mice with either GW4064 or GSK2324, and this effect was specific as it was not observed in *Fxr*^{-/-} mice treated with either agonist (Fig. 2E).

In order to determine whether cholic acid, an endogenous ligand that activates a number of receptors, including FXR (Makishima et al., 1999; Parks et al., 1999), induces these same genes, we fed wild-type and *Fxr*^{-/-} mice (KO) a diet containing non-toxic levels of cholic acid (0.2%) for 7 days. The hepatic expression of *MafG* and *Zfp385a* (Fig. 2F), as well as the positive controls *Bsep* (Fig. 2F) and *Shp* (Fig. S1D) were modestly induced when wild-type, but not *Fxr*^{-/-} mice, were fed the cholic acid-enriched diet. In contrast, the increase in *Crip2* mRNA levels did not reach statistical significance (Fig. 2F). Taken together these results demonstrate that *MafG*, *Crip2* and *Zfp385a*, that encode putative transcriptional repressors, are induced by specific FXR agonists (GSK2324 and GW4064), while *MafG* and *Zfp385a* are also induced by cholic acid, an endogenous FXR ligand.

To determine the optimal dose of GSK2324, we treated wild-type mice for 3 days with vehicle, or 10, 30 or 100mpk GSK2324. Induction of the classic FXR target genes *Shp* and *Bsep* was dependent upon the dose of GSK2324 with near-maximal effects at 30mpk (Fig. S2A). Induction of *Crip2*, *MafG* and *Zfp385a* was also dependent upon the dose of GSK2324 (Fig. 2G). Further, a single dose of GSK2324 at 30mpk resulted in a significant induction of *Crip2*, *MafG* and *Zfp385a* (Fig. 2H) and *Shp* and *Bsep* (Fig. S2B) mRNA levels within one hour. To investigate whether induction of *Crip2*, *MafG* and *Zfp385a* in response to GSK2324 is dependent upon hepatic FXR expression, we treated wild-type (*Fxr*^{fllox/fllox}) mice or littermates lacking hepatic *Fxr* (*Fxr*^{L-/L-}; L-KO) for 3 days with the agonist at 30mpk. While GSK2324 treatment of *Fxr*^{fllox/fllox} mice led to increased hepatic expression of *Crip2*, *MafG*, *Zfp385a* and *Shp*, induction of these genes was not observed following GSK2324 treatment of *Fxr*^{L-/L-} mice (Fig. 2I; Fig. S2C). Taken together, our results demonstrate that *Crip2*, *MafG* and *Zfp385a* are acutely and robustly induced following activation of hepatic FXR.

***MafG* Overexpression *in vivo* Decreases *Cyp8b1* and Biliary Cholic Acid Levels**

To investigate the potential repressive effects of *MafG*, *Crip2*, and *Zfp385a* on gene expression, we generated, and then injected, adenoviral vectors to acutely overexpress these three proteins in the livers of wild-type mice. We then measured the hepatic mRNAs of the two major bile acid synthetic enzymes as these are robustly repressed following activation of FXR (Fig. 1B). Ad-*MafG*, but not Ad-*Crip2* or Ad-*Zfp385a* treatment, resulted in a decrease in the hepatic levels of *Cyp8b1* (Fig. 3A). In contrast, the expression of *Cyp7a1* was unaffected by any of these treatments (Fig. 3A).

The MafG-dependent repression of *Cyp8b1* suggests that MAFG may regulate the synthesis of cholic acid, and alter the bile acid pool composition. To determine whether MAFG overexpression could indeed change the biliary pool composition, we treated a new cohort of mice with either Ad-control or Ad-MafG adenovirus. Changes in the composition of the bile acid pool are relatively slow under normal conditions since only 5% of the bile acids are excreted each day during multiple enterohepatic cycles (de Aguiar Vallim et al., 2013a; Hofmann and Hagey, 2008). Consequently, we fed mice either control diet (chow), or the same diet supplemented with a bile acid sequestrant (0.25% Colesevelam/Welchol) for 7 days prior to treatment with Ad-control or Ad-MafG. Bile acid sequestrants bind bile acids in the intestine, preventing their re-absorption in the ileum and promoting bile acid excretion in the feces (Hofmann and Hagey, 2008). The result is impaired enterohepatic re-circulation of bile acids, de-repression of genes involved in bile acid synthesis and changes in the bile acid pool size (Hofmann and Hagey, 2008; Kong et al., 2012). As expected, Ad-MafG increased the hepatic expression of MAFG mRNA (Fig. 3B) and protein (Fig. 3C and full blot in Fig. S2D), regardless of the presence or absence of the bile acid sequestrant in the diet. The bile acid sequestrant-containing diet increased basal expression of *Cyp8b1*, as expected (Fig. 3D). Importantly, Ad-MafG treatment of both the control and Colesevelam-fed mice resulted in a significant repression *Cyp8b1* mRNA (Fig. 3D). Consistent with this decrease in *Cyp8b1* mRNA, we observed a concomitant decrease in cholic acid and an increase in muricholic acid levels in the bile of Ad-MafG-treated mice (Fig. 3E). Moreover, the MafG-dependent changes in bile acids were qualitative, not quantitative, as total bile acid levels in the liver, intestine or gall bladder (Fig. S2E–G) were similar in mice treated with Ad-control, Ad-MafG, Ad-Crip2 or Ad-Zfp385a. Thus, these two studies demonstrate that the *MafG*-dependent repression of *Cyp8b1* is sufficient to decrease cholic acid and increase muricholic acid levels, even after acute (7 days) and modest increases (2–3 fold) in MAFG protein.

To determine whether the pathway described here is conserved in human cells, we treated the human hepatoma cell line HepG2 with increasing concentrations of CDCA, a natural FXR agonist (Makishima et al., 1999; Parks et al., 1999). Consistent with our observations in mouse liver, CDCA treatment increased the expression of both *MAFG* (Fig. 3F) and *SHP* (Fig. S2H). As expected, CDCA treatment also decreased *CYP7A1* and *CYP8B1* expression in dose-dependent manner (Fig. 3G). Finally, Ad-MafG, but not Ad-Crip2 or Ad-Zfp385a treatment of HepG2 cells decreased *CYP8B1* expression without affecting *CYP7A1* (Fig. 3H). Thus, we have identified a pathway whereby MAFG represses *CYP8B1* expression both in mice, and in human cells.

To further characterize the FXR-dependent regulation of *MafG*, we carried out more in depth analysis. The *MafG* gene is reported to contain two transcriptional start sites that correspond to exon 1a or exon 1b (Katsuoka et al., 2005a) (Fig. 3I). However, our analysis of hepatic RNA-Seq data from Menet *et al.* (Menet et al., 2012) (Fig. 3I, upper panel) together with the data of Katsuoko *et al.* (Katsuoka et al., 2005a) suggest that in the liver, *MafG* is preferentially transcribed from exon 1b (Fig. 3I). Thus, the putative FXRE identified by ChIP-Seq analysis (Fig. 2B) would reside in the hepatic *MafG* proximal promoter that lies upstream of exon 1b (Fig. 3I). Consequently, we generated a luciferase

reporter gene controlled by the hepatic *MafG* promoter (upstream of exon 1b). Treatment of cells with GSK2324, following co-transfection of plasmids expressing FXR and the reporter gene, led to a robust increase in luciferase activity (Fig. 3J). In contrast, the FXR- and GSK2324-dependent increase in luciferase activity was abolished when the FXRE, which corresponds to an inverted repeat 1 (IR-1), was mutated in the *MafG* promoter construct (Fig. 3J). Taken together, these data demonstrate that *MafG* is a *bone fide* FXR target gene that contains a functional FXRE in its hepatic proximal promoter.

MAFG Overexpression in Mouse Liver Represses Numerous Genes Involved in Bile Acid Metabolism

MAFG is a member of the small MAF family of transcription factors, composed of MAFG, MAFF and MAFK, which lack an activation domain and therefore are considered transcriptional repressors (Motohashi et al., 2002). Small MAF proteins can bind to DNA as either homo- or hetero-dimers and function as transcriptional repressors. Alternatively, they can heterodimerize with transcriptional activators to induce gene expression (Motohashi et al., 2002). Consistent with their role as transcription factors, we show that epitope-tagged MAFG localizes to the nucleus (Fig. S3A). *MafG* is expressed in several metabolic tissues, including the liver (Fig. S3B), the major site for bile acid synthesis.

To determine if MAFG overexpression regulated additional genes of bile acid metabolism, in addition to *Cyp8b1*, we carried out gene expression profiling of livers of mice treated with either control or *MafG* adenovirus (Fig. 4A). MAFG overexpression repressed 554 genes and activated 833 genes. Induction of genes in response to MAFG overexpression is not unexpected, as MAFG can heterodimerize with transcriptional activators, most notably NRF2 and NRF3, to activate specific genes (Katsuoka et al., 2005a; Katsuoka et al., 2005b). Gene ontology analysis (Huang da et al., 2009) of the hepatic genes that are repressed following MAFG overexpression revealed a significant enrichment in primary bile acid synthesis genes (Fig. 4B) that included *Cyp8b1* and *Cyp7b1*, as well as the bile acid importer, sodium taurocholate co-transporting polypeptide (*Ntcp*, gene symbol *Slc10a1*). Interestingly, these same genes are also repressed in mouse liver following treatment with FXR agonists (Fig. 1B–D) suggesting that the repression of these genes by FXR agonists is indirect and likely dependent upon induction of MAFG mRNA and protein levels.

We also determined the expression of the remaining bile acid synthesis genes in Ad-control and Ad-MafG treated mice that had been fed either normal chow or a diet supplemented with 0.25% Colesevelam. Ad-MafG treatment resulted in repression of almost all bile acid synthesis genes, including *Cyp7b1*, *Cyp27a1*, independent of the diet (Fig. 4C). Interestingly, comparison of the data shown in Figs. 4C and 1D demonstrates that the bile acid synthetic genes that are repressed following FXR activation are also repressed following overexpression of MAFG. The repression of bile acid synthesis genes is not universal, since *Amacr* and *Cyp39a1* mRNA levels were unchanged following treatment of mice with FXR agonists or following hepatic overexpression of MAFG (Figs. 1D and 4C). Together, these data suggest that MAFG is an important transcriptional regulator of bile acid synthesis and may play an important role in mediating the FXR dependent repression of genes involved in bile acid metabolism.

Loss of MAFG Causes De-repression of Multiple Bile Acid Synthetic Genes and Increases Biliary Cholic Acid Levels

To further evaluate the role of *MafG* in regulating bile acid metabolism, we investigated the effect of loss of *MafG*. Short-term silencing of *MafG* in isolated mouse hepatocytes using three distinct shRNA constructs (Fig. 5A) resulted in de-repression of *Cyp8b1* (Fig. 5B). Further, siRNA-mediated silencing of MAFG mRNA and protein levels in human HepG2 cells (Fig. 5C), also led to de-repression of *CYP8B1* (Fig. 5D). Together, these results suggest *MafG* is a critical negative regulator of *Cyp8b1* expression in both mice and humans. We then generated an antisense oligonucleotide (ASO) to silence *MafG* *in vivo*. Acute treatment with the *MafG* ASO significantly decreased the levels of *MafG* mRNA (Fig. 5E) and protein (Fig. 5F, full blot in S4A). Notably, *Cyp8b1*, but not *Cyp7a1*, was de-repressed in mice after *MafG* silencing with the ASO treatment (Fig. 5G), thus recapitulating our *in vitro* findings in an *in vivo* setting.

To determine whether complete loss of *MafG* also affected bile acid homeostasis we obtained *MafG*^{+/-} mice, which are reported to generate viable *MafG*^{-/-} mice on a mixed background (Shavit et al., 1998). We then backcrossed *MafG*^{+/-} mice onto a C57BL/6 background for 10 generations to be consistent with the genetic background of all other mice used in the current studies. Unexpectedly, we failed to recover any *MafG*^{-/-} mice on a C57BL/6 background (data not shown). We conclude that complete loss of *MafG* on a C57BL/6 background is lethal, likely a result of pronounced neurological disorders previously reported in *MafG*^{-/-} mice on a mixed genetic background (Shavit et al., 1998). Consequently our studies are limited to heterozygous *MafG*^{+/-} mice and their wild-type littermates. As expected, hepatic *MafG* mRNA and protein levels are decreased approximately 50% in *MafG*^{+/-} mice (Fig. 5H). Importantly, *Cyp8b1*, but not *Cyp7a1* mRNA levels were induced/de-repressed in the *MafG*^{+/-} mouse liver (Fig. 5I). Other genes, such as *Cyp7b1*, *Cyp27a1* that we have shown are repressed following *MafG* overexpression (Fig. 4C), were also de-repressed in the livers of chow-fed *MafG*^{+/-} mice (Fig. 5I). Importantly, partial loss of *MafG* mRNA and protein led to a significant increase in the biliary levels of cholic acid, and decreased muricholic acid levels in *MafG*^{+/-} mice (Fig. 5J) consistent with de-repression of *Cyp8b1*. *MafG*^{+/-} mice do not have significantly altered total bile acid levels in liver, intestine or gall bladder (Fig. S4B–D), suggesting MAFG regulates the bile acid pool composition, but not the pool size. We quantified the expression of multiple genes encoding enzymes of the bile acid synthetic pathway in the livers of wild-type and *MafG*^{+/-} mice. Partial loss of MAFG caused de-repression of several genes, including *Acox2*, *Akr1d1*, *Akr1c14*, *Hsd17b4*, *Ntcp* and *Scp2* (Fig. 5K). Collectively these results support the hypothesis that hepatic MAFG functions as a repressor of *Cyp8b1* and cholic acid synthesis as well as a regulator of bile acid metabolism *in vivo*.

Identification of MAFG Binding Sites at Multiple Genes Involved in Bile Acid Synthesis and Metabolism

To investigate the molecular mechanism for the *MafG*-dependent repression of *Cyp8b1* as well as additional target genes, we generated an adenovirus construct to overexpress a biotin-ligase recognition peptide (BLRP)-tagged *MafG*. Consistent with our studies using untagged MAFG (Ad-MafG) (Fig. 3A–D), treatment of mice with Ad-BLRP-MafG resulted

in increased hepatic *MafG* mRNA (Fig. S5A) and protein (Fig. 6A) and decreased *Cyp8b1*, *Cyp7b1* and *Cyp27a1* expression (Fig. S5B), suggesting the BLRP epitope does not interfere with MAFG function. We then used ChIP analysis to identify MAFG bound to MAFG response elements (MAREs). First, as controls we show that in mouse liver, BLRP-tagged MAFG was enriched at MAREs that had been previously identified in *Nqo* and *G6pdx* in studies using cultured cells (Hirotsu et al., 2012) (Fig. S5C). We then carried out ChIP-Seq analysis from livers of mice treated with Ad-BLRP-MafG as well as Ad-BLRP (control), using the same anti-BLRP antibody. Global analysis of all peaks for MAFG revealed 46% reside in intergenic regions, as compared to 41% in introns, while there was a modest enrichment in proximal promoters (Fig. 6B). Motif enrichment analysis of sequences for the top 20,000 MAFG peaks (representing the largest number of reads per site) identified the consensus MARE (Fig. 6C, top). This sequence is highly similar to the MARE described previously for MAFG homodimers (Hirotsu et al., 2012). Analysis of all MAFG ChIP-Seq peaks ($n = 68,754$) identified a MARE that contained a consensus sequence of GTCAGC (Fig. 6C, bottom), but was otherwise different from that found in the top 20,000 peaks. Presumably, the latter MARE represents various binding sites for complexes containing different MAFG-containing heterodimers. The MARE motif identified in the top MAFG 20,000 peaks was present in 59% of all peaks, whereas the same motif was present in 4% of the Ad-BLRP-control (Fig. 6C). Similarly, analysis for all 68,754 peaks identified the different MARE motif in 42% of peaks, compared to 4% in the background control (Fig. 6C).

We next searched the *Cyp8b1* locus of the MAFG ChIP-Seq data. This identified a number of MAREs within 10kb of the *Cyp8b1* gene (Fig. 6D, lower panel), and one peak present near the transcriptional start site (TSS). We confirmed the enrichment of MAFG in the *Cyp8b1* proximal promoter by RT-qPCR ChIP analysis (Fig. 6E). Complementary analysis of the *Cyp8b1* promoter (0.5kb) using luciferase reporter assays demonstrated a dose-dependent repression following MAFG overexpression (Fig. 6F). In contrast, mutation of the MARE within the *Cyp8b1* promoter resulted in de-repression of the luciferase reporter gene, which was no longer repressed by MAFG overexpression (Fig. 6F). These results demonstrate direct binding of MAFG to multiple sites upstream of *Cyp8b1*, and to one site in the proximal promoter, that identify the molecular mechanism for the MAFG-dependent repression of *Cyp8b1*.

MAFG ChIP-Seq analysis also identified MAREs in the promoter and/or intronic regions of *Cyp27a1* (Fig. 6G, lower panel) and *Cyp7b1* (Fig. 6H, lower panel). In contrast, peaks for MAFG binding sites were not present in ChIP-Seq data from mice treated with the control Ad-BLRP (Fig. 6D, G-H, upper panels). Analysis of the proximal *Cyp7b1* promoter using a luciferase reporter gene showed that MAFG overexpression reduced luciferase activity in a dose-dependent manner (Fig. 6I). Further, we also identified MAREs in several other bile acid synthetic genes, including *Acox2*, *Akr1d1*, *Akr1c14*, *Ntcp*, *Hsd17b4* and *Scp2* (Fig. S5D–I), but not in the 100kb upstream of *Cyp7a1* (Fig. S5J). Together, these data demonstrate that MAFG directly regulates several bile acid metabolism genes.

Interestingly, liver-specific LRH-1 deficient mice also have decreased *Cyp8b1*, unchanged *Cyp7a1* and altered bile acid composition (Lee et al., 2008; Matakai et al., 2007). We

therefore investigated whether MAFG binding sites were associated with LRH-1 occupancy in the liver. Using ChIP-Seq analysis for hepatic LRH-1 sites (Chong et al., 2012), we only identified a small number of genes that had both MAFG and LRH-1 binding sites (282 of 10,351; Fig S6A), and these genes were enriched in genes of negative regulation of metabolic processes, but not bile acid synthesis genes (Fig. S6B). Taken together, these results suggest MAFG is unlikely to repress transcription of multiple bile acid synthetic genes by displacing LRH-1.

In conclusion, our extensive studies identify a pathway involving the nuclear receptor FXR and the FXR-target gene *MafG* that functions to repress transcription of *Cyp8b1*, as well as multiple bile acid genes including *Acox2*, *Akr1d1*, *Akr1c14*, *Cyp7b1*, *Cyp27a1*, *Hsd17c14*, *Ntcp* and *Scp2* and thus modulate bile acid homeostasis (Fig. 7).

Discussion

The current studies identify an FXR-MAFG pathway that controls the transcription of multiple genes involved in both the classic and alternative pathways of bile acid synthesis, and bile acid transport. We show that the *MafG* gene is a direct target of FXR, and that MAFG subsequently represses many genes involved in bile acid synthesis and metabolism (Figs. 1–4, Fig. 7). Further, we show that loss of 50% hepatic MAFG leads to de-repression of many of these genes (Fig. 5). Importantly, we demonstrate that MAFG binds to MAREs associated with the same repressed genes (Fig. 6–Fig. 7). *Cyp8b1* or *Cyp7b1* promoter-reporter assays provided additional insight into the functional importance of selected MAREs (Fig. 6). The identification of a MAFG-dependent regulation of *Cyp8b1*, *Acox2*, *Akr1d1*, *Akr1c14*, *Cyp27a1*, *Cyp7b1*, *Hsd17c4*, *Ntcp* and *Scp2* suggests a concerted action of MAFG in regulating various aspects of bile acid metabolism that has not been previously appreciated (Fig. 1A).

Consistent with the finding that hepatic overexpression of MAFG in mice represses *Cyp8b1*, we show that under these conditions there is a decrease in biliary cholic acid and an increase in muricholic acid levels (Fig. 3), without increasing bile acid levels in liver, intestine or gall bladder (Fig. S2E–G). This finding is consistent with *Cyp8b1* encoding the regulatory enzyme for cholic acid synthesis from 7-hydroxycholesterol, and the earlier observation that *Cyp8b1*^{-/-} mice not only fail to synthesize cholic acid but exhibit increased muricholic acid levels in bile, without a change in the bile acid pool size (Li-Hawkins et al., 2002). In contrast, loss of MAFG, as a result of partial gene ablation or silencing, caused de-repression of *Cyp8b1* (Fig. 5), and an increased ratio of cholic acid:muricholic acid without altering total bile acid levels in liver, intestine and gall bladder (Fig. S4B–D). This change in the bile acid composition is expected to alter the hydrophobicity. However, the physiologic consequences of such a change on metabolism as a whole are unknown and will require additional studies.

We did not observe changes in *Cyp7a1* mRNA levels in the *MafG*^{+/-} mice or in ASO treated wild-type mice (Fig. 5), further supporting the specificity of the regulation of specific bile acid genes by MAFG. Nonetheless, after prolonged MAFG overexpression, we have observed some repression of *Cyp7a1* (data not shown). This effect was not consistent across

all our studies. Since *MafG* silencing and *MafG*^{+/-} mice do not exhibit changes in *Cyp7a1* expression (Fig. 5) and MAFG ChIP-Seq analysis at the *Cyp7a1* locus did not identify MAFG binding sites (Fig. S5J), we suggest that the repression of *Cyp7a1* may be indirect.

The current studies suggest that MAFG represents a complimentary pathway that is critical for the regulation of bile acid homeostasis. Previous studies reported that the FXR-dependent regulation of *Cyp8b1* involves *Shp* (Kerr et al., 2002; Wang et al., 2002), although the authors suggested at that time that additional unknown pathways were likely to play a role in the repression of bile acid synthetic genes. Earlier *in vitro* studies had shown that SHP can repress luciferase reporter gene activity by binding to and inhibiting HNF4a and LRH-1 transcription factors that normally activate *Cyp7a1* and/or *Cyp8b1* (Goodwin et al., 2000; Lu et al., 2000). Nonetheless, the effects of hepatic overexpression of SHP on the expression of *Cyp7a1* or *Cyp8b1* *in vivo* are at best very modest (Kir et al., 2012; Kong et al., 2012), while the effects of SHP overexpression on other bile acid synthetic genes or bile acid composition have not been reported. Further, Kong *et al.*, reported that treatment of *Shp*^{-/-} mice with the FXR agonist GW4064 resulted in near normal repression of both *Cyp8b1* and *Cyp7a1* (Kong et al., 2012). Taken together, these results contrast with the broad and significant repression of numerous bile acid synthetic genes and the decreased levels of cholic acid we observe in mice following MAFG overexpression (Figs. 3 and 5).

A second pathway that leads to repression of *Cyp7a1* involves activation of FXR in enterocytes and the resulting increase in *Fgf15* (mouse) or *FGF19* (humans) and subsequent secretion of the protein (Inagaki et al., 2005). FGF15/19 binds to the cognate receptor, FGFR4/β-klotho, resulting in repression of *Cyp7a1* (Potthoff et al., 2012). Whether the FGF15/19 pathway plays a role in the regulation of *Cyp8b1* is unclear at the present time. A recent study also demonstrated a co-requirement for SHP in mediating the effects of FGF19 repression of *Cyp7a1* (Kir et al., 2012). In contrast, a separate study showed that injection of FGF15 protein into *Shp*^{-/-} mice resulted in near normal repression of both *Cyp7a1* and *Cyp8b1* (Kong et al., 2012). Thus, it appears that the precise role of SHP in mediating the FGF15/19 and/or FXR-dependent repression of *Cyp8b1* and/or *Cyp7a1* remains to be established. Nonetheless, the finding that *Cyp7a1* and/or *Cyp8b1* mRNA levels are induced/de-repressed in cells or the livers of mice deficient for either *Shp* (Kerr et al., 2002; Wang et al., 2002), *Fgfr4/j3-klotho* (Kong et al., 2012) or *MafG* (Fig. 5) suggest that SHP, FGF15/19 and MAFG represent three complimentary pathways that control bile acid synthesis and composition. Indeed, the existence and complexity of the complementary pathways highlight the fact that tight regulation of bile acid homeostasis is required, and dysregulation can lead to various metabolic diseases.

The role of MAFG in bile acid metabolism has not been previously appreciated. The MAF family of proteins is divided into small (MAFG, MAFF and MAFK) and large (cMAF, MAFA, MAFB) members (Kannan et al., 2012). The small members contain a DNA-binding domain and a basic leucine zipper, but lack the transcriptional activation domain found in the large family members (Kannan et al., 2012; Motohashi et al., 2002). Small members of the family can form homodimers or heterodimers that bind MAF-response elements (MAREs) to repress transcription of target genes (Kurokawa et al., 2009). However, the small MAF proteins can also dimerize with transcriptional activators, such as NRF2, a

member of the Cap 'n' Collar family of transcription factors, to induce genes involved in the stress response and detoxification (Kannan et al., 2012; Motohashi et al., 2002). At the current time, the factors that control the formation of homodimers versus heterodimers of the small MAF proteins are poorly understood.

Feedback repression of bile acid synthesis in response to accumulating bile acids is critical for the normal maintenance of bile acid homeostasis and for the prevention of hepatotoxicity that occurs with elevated levels of bile acids. The identification of the pathway described here may have important implications in disease since bile acid metabolism is linked to several metabolic disorders including cardiovascular, diabetes, as well as specific types of cancer.

Experimental Procedures

GSK2324 was dissolved in water and administered to mice via intraperitoneal injection (I.P.) at 30mg/kg body weight (mpk) unless otherwise stated. In experiments where GW4064 and GSK2324 were compared, agonists were dissolved in water containing 0.5% Tween 80, and mice were treated once daily with either drug or vehicle alone at 60mpk for 3 days via I.P. injection. Unless otherwise stated, mice were fasted for 4–6 hours after the last treatment with FXR agonists prior to removal of tissues. All animal experiments were carried out according to NIH guidelines and were approved by the Office of Animal Research Oversight (OARO) at UCLA. For MafG ASO studies, male 12-week old C57BL/6 mice (Jackson Laboratories) were dosed once with either control or MafG ASO at 100mpk and 3 days later, mice were fasted overnight and livers collected the following morning (9–11am). All adenoviruses were prepared in BSL2 category facilities. Briefly, cDNAs for mouse *MafG*, *Crip2*, *Zfp385a* were cloned from whole liver cDNA into pAdTrack CMV plasmid, and prepared as described in (Bennett et al., 2013). For animal experiments, 1×10^9 PFU were used, and tissues collected after 5–7 days, and for cell culture studies, an MOI of 1–10 was used and cells harvested for analysis after 24–48 hours. For gene expression analysis, RNA was isolated using QIAzol according to manufacturers instructions (Qiagen) and rDNaseI treated before complementary DNA was synthesized (Life Technologies). RT-qPCR analysis was carried out using primers described in Supplemental Table I and gene expression data was normalized to *Tbp* and/or *36B4/Rplp0*. Western blotting analysis was carried out from liver samples (approximately 100mg of tissue) were homogenized in 1ml of RIPA buffer supplemented with protease inhibitor complex (Roche). Protein was quantified using the BCA assay (ThermoFisher) and 10–30ng of protein was loaded on pre-cast gels (BioRad). Protein was transferred to PVDF membranes (Millipore), probed with antibodies described in Extended Experimental Procedures and detected ECL reagent (Sigma) or ECL Prime (GE Healthcare) using a GE Image Quant LAS 4000 detection system (GE Healthcare). Bile acid analysis was carried out from biliary material by HPLC, and the major taurine-conjugated species were detected by measuring absorbance measured at 205nm and compared to known bile acid standards. Total bile acids were measured in liver, intestine and gall bladder as described in in Extended Experimental Procedures. For promoter-reporter studies, mouse *MafG* promoter (2kb), *Cyp8b1* promoter (0.5kb) and *Cyp7b1* promoter (1kb) were amplified from mouse genomic DNA (C57BL/6) using KAPA HiFi polymerase (Kapa) and cloned into pGL4.10[luc2] plasmid (Promega).

Luciferase reporter constructs were transfected using Fugene HD (Promega) (n=6 wells per condition) according to manufacturer's instructions into human HepG2 or Hep3B cells (ATCC), plated onto 48-well dishes. For MafG ChIP analysis, mice were treated with Ad-BLRP or Ad-BLRP-MafG for 5 days. Livers were fixed in PBS containing 1% formaldehyde, nuclei were isolated, chromatin was sheared by sonication for 25–30 cycles using BioRuptor Twin (Daigenode) and immunoprecipitated using a BLRP antibody (Avitag, GeneScript) as described in the Extended Experimental Procedures. For ChIP-Seq, immunoprecipitated DNA was used for library preparation (Kapa Biosystems) and sequenced by the UCLA UNG Core. Analysis of ChIP- and RNA-Seq as well as microarray analysis are described in the Extended Experimental Procedures.

Statistics

All bars shown are mean \pm S.E.M. The comparison of different groups was carried out with Student's t test, one- and two-way ANOVA, and differences under $p < 0.05$ were considered statistically significant (* $p < 0.05$, ** $p < 0.01$, *** $p < 0.001$, and different letters indicate at least $p < 0.05$).

Supplementary Material

Refer to Web version on PubMed Central for supplementary material.

Acknowledgements

We thank Drs Timothy Willson and David Deaton for the kind gift of GSK2324, and Peter Tontonoz and his lab for helpful discussions. We also thank Tieyan Han, Joan Cheng, Christina Cheung and Elizabeth Nam for excellent technical assistance. This work was supported in part by United States Public Health Service, grants 1R01DK102559-01 and the Laubish fund at UCLA (to P.A.E.); American Heart Association (AHA) Beginning Grant In Aid (13BGIA17080038) and NIH K99HL118161 (to E.J.T); AHA Postdoctoral Fellowship (12POST11760017) and NIH NHLBI K99HL12348501 (to C.E.R); T.Q. de A.V. was supported by an AHA Scientist Development Grant (14SDG18440015), NIH P30 DK 41301 and P30 DK063491 and UCLA Clinical and Translational Science Institute (CTSI) UL1TR000124.

References

- Ananthanarayanan M, Balasubramanian N, Makishima M, Mangelsdorf DJ, Suchy FJ. Human bile salt export pump promoter is transactivated by the farnesoid X receptor/bile acid receptor. *J Biol Chem.* 2001; 276:28857–28865. [PubMed: 11387316]
- Bass JY, Caravella JA, Chen L, Creech KL, Deaton DN, Madauss KP, Marr HB, McFadyen RB, Miller AB, Mills WY, et al. Conformationally constrained farnesoid X receptor (FXR) agonists: heteroaryl replacements of the naphthalene. *Bioorg Med Chem Lett.* 2011; 21:1206–1213. [PubMed: 21256005]
- Bavner A, Sanyal S, Gustafsson JA, Treuter E. Transcriptional corepression by SHP: molecular mechanisms and physiological consequences. *Trends Endocrinol Metab.* 2005; 16:478–488. [PubMed: 16275121]
- Beher WT, Baker GD, Anthony WL, Beher ME. The feedback control of cholesterol biosynthesis. *Henry Ford Hosp Med Bull.* 1961; 9:201–213. [PubMed: 13688687]
- Bennett BJ, Vallim TQdA, Wang Z, Shih D, Meng Y, Gregory J, Allayee H, Lee R, Graham M, Crooke R, et al. Genetic and Dietary Regulation of Trimethylamine-N-Oxide, a Metabolite Associated with Atherosclerosis. *Cell Metab.* 2013; 17:49–60. [PubMed: 23312283]
- Chong HK, Biesinger J, Seo YK, Xie X, Osborne TF. Genome-wide analysis of hepatic LRH-1 reveals a promoter binding preference and suggests a role in regulating genes of lipid metabolism in concert with FXR. *BMC Genomics.* 2012; 13:51. [PubMed: 22296850]

- Chong HK, Infante AM, Seo YK, Jeon TI, Zhang Y, Edwards PA, Xie X, Osborne TF. Genome-wide interrogation of hepatic FXR reveals an asymmetric IR-1 motif and synergy with LRH-1. *Nucleic Acids Res.* 2010; 38:6007–6017. [PubMed: 20483916]
- de Aguiar Vallim TQ, Tarling EJ, Edwards PA. Pleiotropic roles of bile acids in metabolism. *Cell Metab.* 2013a; 17:657–669. [PubMed: 23602448]
- de Aguiar Vallim TQ, Tarling EJ, Kim T, Civelek M, Baldan A, Esau C, Edwards PA. MicroRNA-144 regulates hepatic ATP binding cassette transporter A1 and plasma high-density lipoprotein after activation of the nuclear receptor farnesoid X receptor. *Circ Res.* 2013b; 112:1602–1612. [PubMed: 23519696]
- Duran-Sandoval D, Cariou B, Percevault F, Hennuyer N, Grefhorst A, van Dijk TH, Gonzalez FJ, Fruchart JC, Kuipers F, Staels B. The farnesoid X receptor modulates hepatic carbohydrate metabolism during the fasting-refeeding transition. *J Biol Chem.* 2005; 280:29971–29979. [PubMed: 15899888]
- Evans RM, Mangelsdorf DJ. Nuclear Receptors, RXR, and the Big Bang. *Cell.* 2014; 157:255–266. [PubMed: 24679540]
- Goodwin B, Jones SA, Price RR, Watson MA, McKee DD, Moore LB, Galardi C, Wilson JG, Lewis MC, Roth ME, et al. A regulatory cascade of the nuclear receptors FXR, SHP-1, and LRH-1 represses bile acid biosynthesis. *Mol Cell.* 2000; 6:517–526. [PubMed: 11030332]
- Hirotsu Y, Katsuoka F, Funayama R, Nagashima T, Nishida Y, Nakayama K, Engel JD, Yamamoto M. Nrf2-MafG heterodimers contribute globally to antioxidant and metabolic networks. *Nucleic Acids Res.* 2012; 40:10228–10239. [PubMed: 22965115]
- Hofmann AF, Hagey LR. Bile acids: chemistry, pathochemistry, biology, pathobiology, and therapeutics. *Cell Mol Life Sci.* 2008; 65:2461–2483. [PubMed: 18488143]
- Huang da W, Sherman BT, Lempicki RA. Systematic and integrative analysis of large gene lists using DAVID bioinformatics resources. *Nat Protoc.* 2009; 4:44–57. [PubMed: 19131956]
- Inagaki T, Choi M, Moschetta A, Peng L, Cummins CL, McDonald JG, Luo G, Jones SA, Goodwin B, Richardson JA, et al. Fibroblast growth factor 15 functions as an enterohepatic signal to regulate bile acid homeostasis. *Cell Metab.* 2005; 2:217–225. [PubMed: 16213224]
- Inagaki T, Moschetta A, Lee YK, Peng L, Zhao G, Downes M, Yu RT, Shelton JM, Richardson JA, Repa JJ, et al. Regulation of antibacterial defense in the small intestine by the nuclear bile acid receptor. *Proc Natl Acad Sci U S A.* 2006; 103:3920–3925. [PubMed: 16473946]
- Kannan MB, Solovieva V, Blank V. The small MAF transcription factors MAFF, MAFG and MAFK: Current knowledge and perspectives. *Biochim Biophys Acta.* 2012; 1823:1841–1846. [PubMed: 22721719]
- Katsuoka F, Motohashi H, Engel JD, Yamamoto M. Nrf2 transcriptionally activates the mafG gene through an antioxidant response element. *J Biol Chem.* 2005a; 280:4483–4490. [PubMed: 15574414]
- Katsuoka F, Motohashi H, Ishii T, Aburatani H, Engel JD, Yamamoto M. Genetic evidence that small maf proteins are essential for the activation of antioxidant response element-dependent genes. *Mol Cell Biol.* 2005b; 25:8044–8051. [PubMed: 16135796]
- Kerr TA, Saeki S, Schneider M, Schaefer K, Berdy S, Redder T, Shan B, Russell DW, Schwarz M. Loss of nuclear receptor SHP impairs but does not eliminate negative feedback regulation of bile acid synthesis. *Dev Cell.* 2002; 2:713–720. [PubMed: 12062084]
- Kim I, Ahn SH, Inagaki T, Choi M, Ito S, Guo GL, Kliewer SA, Gonzalez FJ. Differential regulation of bile acid homeostasis by the farnesoid X receptor in liver and intestine. *J Lipid Res.* 2007; 48:2664–2672. [PubMed: 17720959]
- Kir S, Zhang Y, Gerard RD, Kliewer SA, Mangelsdorf DJ. Nuclear receptors HNF4alpha and LRH-1 cooperate in regulating Cyp7a1 in vivo. *J Biol Chem.* 2012; 287:41334–41341. [PubMed: 23038264]
- Kong B, Wang L, Chiang JY, Zhang Y, Klaassen CD, Guo GL. Mechanism of tissue-specific farnesoid X receptor in suppressing the expression of genes in bile-acid synthesis in mice. *Hepatology.* 2012; 56:1034–1043. [PubMed: 22467244]
- Kuipers F, Bloks VW, Groen AK. Beyond intestinal soap-bile acids in metabolic control. *Nat Rev Endocrinol.* 2014; 10:488–498. [PubMed: 24821328]

- Kurokawa H, Motohashi H, Sueno S, Kimura M, Takagawa H, Kanno Y, Yamamoto M, Tanaka T. Structural basis of alternative DNA recognition by Maf transcription factors. *Mol Cell Biol.* 2009; 29:6232–6244. [PubMed: 19797082]
- Lee FY, de Aguiar Vallim TQ, Chong HK, Zhang Y, Liu Y, Jones SA, Osborne TF, Edwards PA. Activation of the farnesoid X receptor provides protection against acetaminophen-induced hepatic toxicity. *Mol Endocrinol.* 2010; 24:1626–1636. [PubMed: 20573685]
- Lee YK, Schmidt DR, Cummins CL, Choi M, Peng L, Zhang Y, Goodwin B, Hammer RE, Mangelsdorf DJ, Kliewer SA. Liver receptor homolog-1 regulates bile acid homeostasis but is not essential for feedback regulation of bile acid synthesis. *Mol Endocrinol.* 2008; 22:1345–1356. [PubMed: 18323469]
- Li F, Jiang C, Krausz KW, Li Y, Albert I, Hao H, Fabre KM, Mitchell JB, Patterson AD, Gonzalez FJ. Microbiome remodelling leads to inhibition of intestinal farnesoid X receptor signalling and decreased obesity. *Nat Commun.* 2013; 4:2384. [PubMed: 24064762]
- Li-Hawkins J, Gafvels M, Olin M, Lund EG, Andersson U, Schuster G, Bjorkhem I, Russell DW, Eggertsen G. Cholic acid mediates negative feedback regulation of bile acid synthesis in mice. *J Clin Invest.* 2002; 110:1191–1200. [PubMed: 12393855]
- Lu TT, Makishima M, Repa JJ, Schoonjans K, Kerr TA, Auwerx J, Mangelsdorf DJ. Molecular basis for feedback regulation of bile acid synthesis by nuclear receptors. *Mol Cell.* 2000; 6:507–515. [PubMed: 11030331]
- Makishima M, Okamoto AY, Repa JJ, Tu H, Learned RM, Luk A, Hull MV, Lustig KD, Mangelsdorf DJ, Shan B. Identification of a nuclear receptor for bile acids. *Science.* 1999; 284:1362–1365. [PubMed: 10334992]
- Maloney PR, Parks DJ, Haffner CD, Fivush AM, Chandra G, Plunket KD, Creech KL, Moore LB, Wilson JG, Lewis MC, et al. Identification of a chemical tool for the orphan nuclear receptor FXR. *J Med Chem.* 2000; 43:2971–2974. [PubMed: 10956205]
- Mataki C, Magnier BC, Houten SM, Annicotte JS, Argmann C, Thomas C, Overmars H, Kulik W, Metzger D, Auwerx J, et al. Compromised intestinal lipid absorption in mice with a liver-specific deficiency of liver receptor homolog 1. *Mol Cell Biol.* 2007; 27:8330–8339. [PubMed: 17908794]
- Menet JS, Rodriguez J, Abruzzi KC, Rosbash M. Nascent-Seq reveals novel features of mouse circadian transcriptional regulation. *Elife.* 2012; 1:e00011. [PubMed: 23150795]
- Motohashi H, O'Connor T, Katsuoka F, Engel JD, Yamamoto M. Integration and diversity of the regulatory network composed of Maf and CNC families of transcription factors. *Gene.* 2002; 294:1–12. [PubMed: 12234662]
- Parks DJ, Blanchard SG, Bledsoe RK, Chandra G, Consler TG, Kliewer SA, Stimmel JB, Wilson TM, Zavacki AM, Moore DD. Bile acids: natural ligands for an orphan nuclear receptor. *Science.* 1999; 284:1365–1368. [PubMed: 10334993]
- Potthoff MJ, Kliewer SA, Mangelsdorf DJ. Endocrine fibroblast growth factors 15/19 and 21: from feast to famine. *Genes Dev.* 2012; 26:312–324. [PubMed: 22302876]
- Ridaura VK, Faith JJ, Rey FE, Cheng J, Duncan AE, Kau AL, Griffin NW, Lombard V, Henrissat B, Bain JR, et al. Gut microbiota from twins discordant for obesity modulate metabolism in mice. *Science.* 2013; 341:1241214. [PubMed: 24009397]
- Russell DW. The enzymes, regulation, and genetics of bile acid synthesis. *Annu Rev Biochem.* 2003; 72:137–174. [PubMed: 12543708]
- Ryan KK, Tremaroli V, Clemmensen C, Kovatcheva-Datchary P, Myronovych A, Karns R, Wilson-Perez HE, Sandoval DA, Kohli R, Backhed F, et al. FXR is a molecular target for the effects of vertical sleeve gastrectomy. *Nature.* 2014; 509:183–188. [PubMed: 24670636]
- Shavit JA, Motohashi H, Onodera K, Akasaka J, Yamamoto M, Engel JD. Impaired megakaryopoiesis and behavioral defects in mafG-null mutant mice. *Genes Dev.* 1998; 12:2164–2174. [PubMed: 9679061]
- Sinal CJ, Tohkin M, Miyata M, Ward JM, Lambert G, Gonzalez FJ. Targeted disruption of the nuclear receptor FXR/BAR impairs bile acid and lipid homeostasis. *Cell.* 2000; 102:731–744. [PubMed: 11030617]

- Thomas AM, Hart SN, Kong B, Fang J, Zhong XB, Guo GL. Genome-wide tissue-specific farnesoid X receptor binding in mouse liver and intestine. *Hepatology*. 2010; 51:1410–1419. [PubMed: 20091679]
- Wang L, Lee YK, Bundman D, Han Y, Thevananther S, Kim CS, Chua SS, Wei P, Heyman RA, Karin M, et al. Redundant pathways for negative feedback regulation of bile acid production. *Dev Cell*. 2002; 2:721–731. [PubMed: 12062085]
- Zhang Y, Lee FY, Barrera G, Lee H, Vales C, Gonzalez FJ, Willson TM, Edwards PA. Activation of the nuclear receptor FXR improves hyperglycemia and hyperlipidemia in diabetic mice. *Proc Natl Acad Sci U S A*. 2006; 103:1006–1011. [PubMed: 16410358]

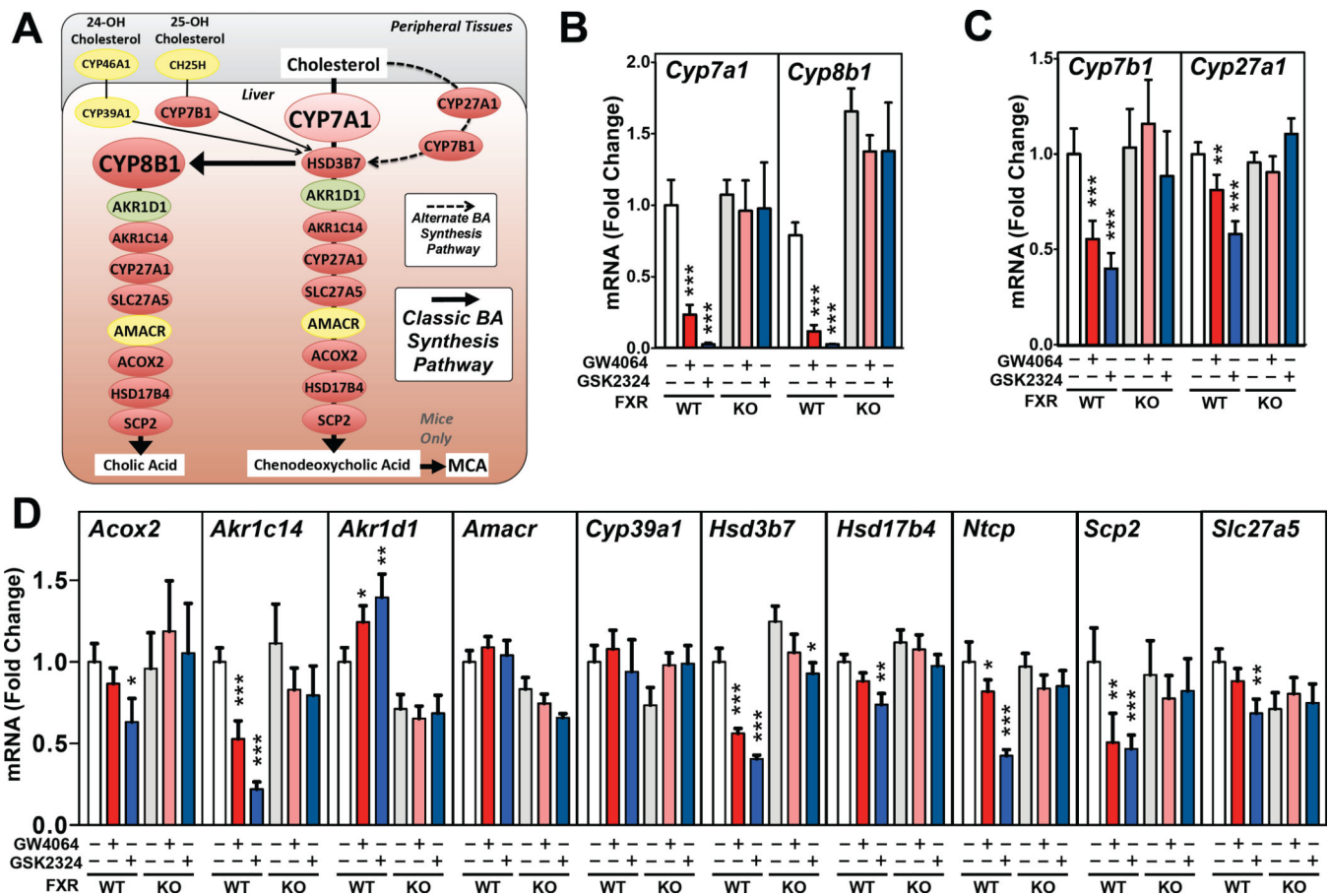


Figure 1. FXR Activation Represses Most Bile Acid Synthesis Genes

(A) Schematic diagram of the major hepatic enzymes involved in bile acid synthesis. Genes in red are repressed, whilst genes in yellow are unchanged and the gene in green is induced following FXR activation. Hepatic expression of genes encoding enzymes of the (B) classic or (C) alternative bile acid synthetic pathway or (D) remaining genes involved in primary bile acid synthesis. mRNA levels were measured by RT-qPCR following treatment of wild-type or *Fxr*^{-/-} mice (7–9 mice/group) for 3 days with GW4064 or GSK2324 at 60mpk/day. All data shown as mean ± SEM. Asterisks indicate statistically significant differences comparing WT or KO vehicle treated against agonist treated mice (* p<0.05; ** p<0.01; *** p<0.001).

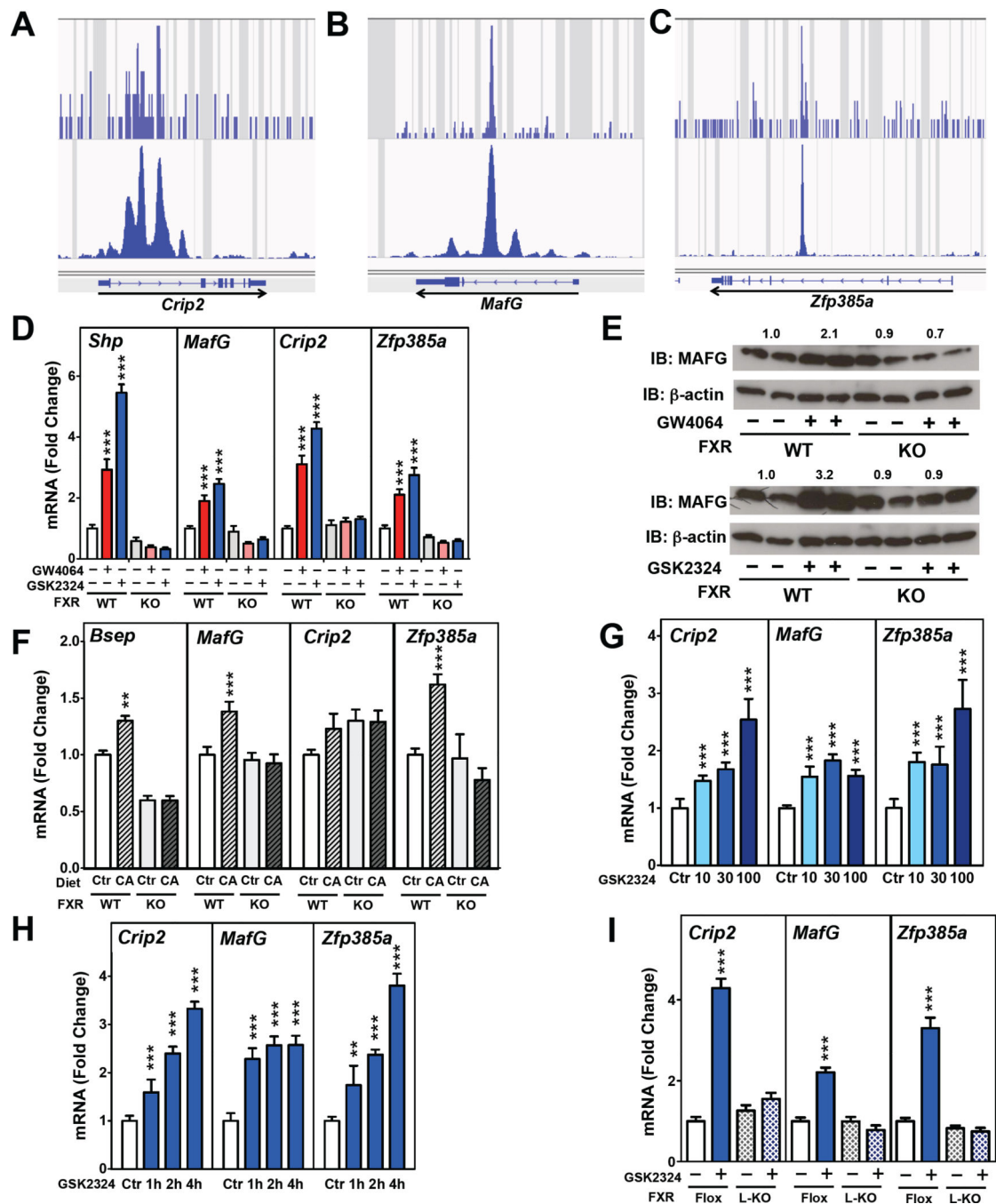


Figure 2. Identification of Transcriptional Repressors as Direct FXR Target Genes

(A–C) ChIP-Seq analysis of hepatic FXR from (Chong et al., 2010) (top) and (Thomas et al., 2010) (bottom) at (A) *Crip2*, (B) *MafG* and (C) *Zfp385a* genomic loci. (D) Hepatic expression of *Shp*, *MafG*, *Crip2*, and *Zfp385a* in C57BL/6 wild-type (WT) and *Fxr*^{-/-} (KO) mice treated with vehicle, GW4064 or GSK2324 for 3 days (n=7–9 mice/group). (E) Western blotting analysis and quantification of MAFG protein in livers of C57BL/6 wild-type and *Fxr*^{-/-} mice treated with vehicle or GW4064 (top), or GSK2324 (bottom) for 3 days. (F) Hepatic expression of *Bsep*, *Crip2*, *MafG* and *Zfp385a* in C57BL/6 wild-type and

Fxr^{-/-} mice fed either a control (Ctr) or 0.2% cholic acid (CA) diet for 7 days. (G) Hepatic expression of *Crip2*, *MafG* and *Zfp385a* in C57BL/6 wild-type mice treated with vehicle (Ctr) or 10, 30 or 100mpk/day of GSK2324 for 3 days (n=4–8 mice/group) or (H) following treatment of wild-type mice with a single injection of GSK2324 (30mpk) 1, 2 or 4h before sacrifice (n=6 mice/group). (I) Hepatic expression of *Crip2*, *MafG* and *Zfp385a* in littermate C57BL/6 wild-type (Flox) or liver-specific *Fxr*^{-/-} mice (L-KO) treated with GSK2324 for 3 days (n=7–9 mice/group). All data shown as mean ± SEM. Asterisks indicate statistically significant differences comparing WT or KO vehicle treated against agonist treated mice (** p<0.01; *** p<0.001).

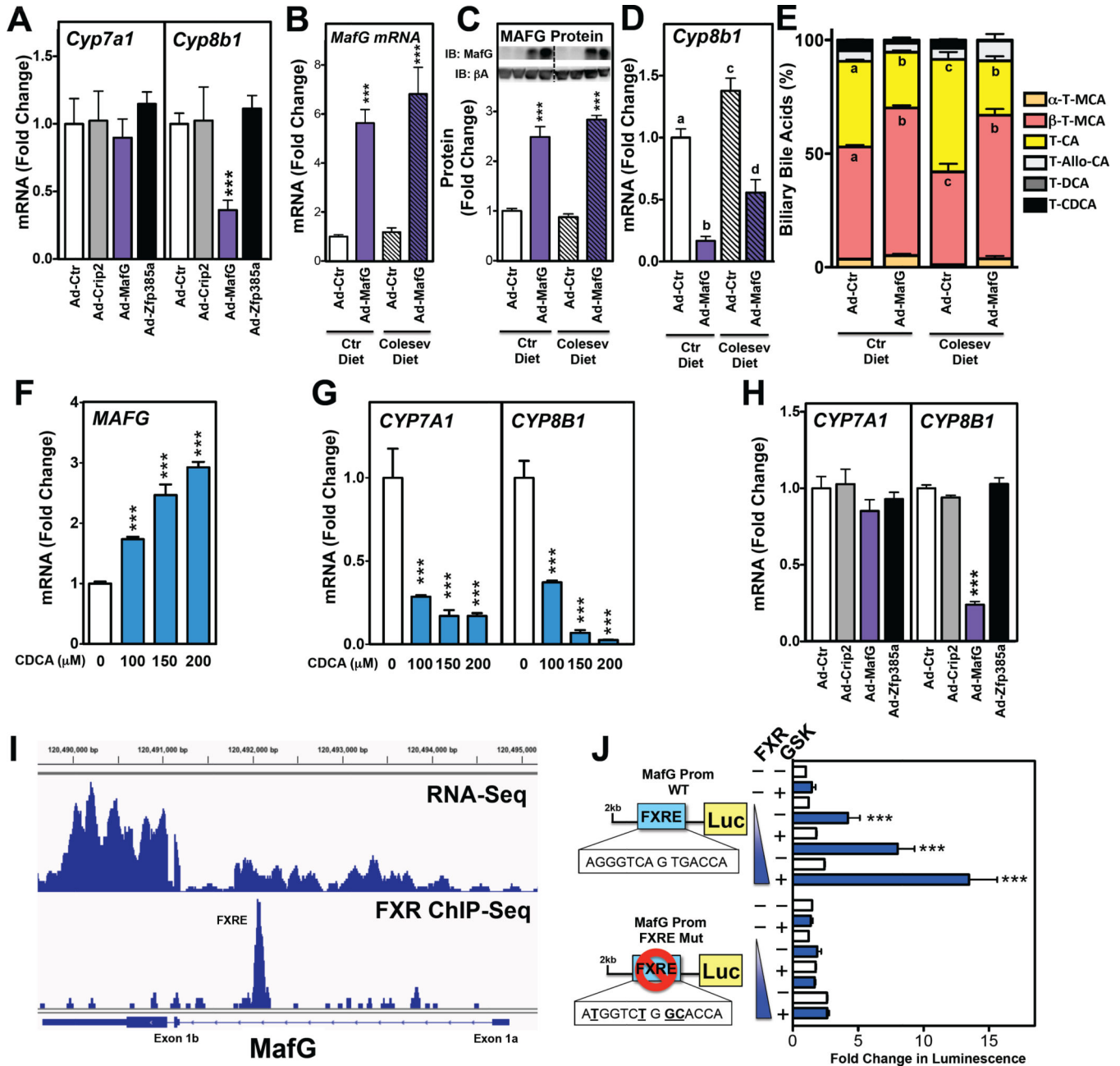


Figure 3. *MafG* Overexpression Represses *Cyp8b1* mRNA and Reduces Biliary Cholic Acid Levels

(A) Hepatic expression of *Cyp7a1* and *Cyp8b1* following treatment of C57BL/6 mice with Ad-control (Ad-Ctr), Ad-Crip2, Ad-MafG or Ad-Zfp385a adenoviruses for 5 days (n=7–8 mice/group). (B–E) Hepatic levels of *MafG* mRNA (B), MAFG protein (C), and *Cyp8b1* mRNA (D) and taurine-conjugated biliary bile acid levels (E) in C57BL/6 wild-type treated with Ad-control or Ad-MafG adenovirus for 7 days and fed either a control or Colesevelam-containing diet (Colesev) for 7 days prior and 7 days post adenovirus treatment (n=8–9 mice/group). (F and G) Expression levels of *MAFG* (F) or *CYP7A1* and *CYP8B1* (G) in human HepG2 cells treated with 100,150 or 200 μ M chenodeoxycholic acid (CDCA) for 24

hours (n=4 wells/condition). (H) Expression levels of *CYP7A1* and *CYP8B1* in HepG2 cells infected with Ad-Control, -Crip2, -MafG or -Zfp385a for 36 hours (n=3–4 wells/condition). (I) RNA-Seq (Menet et al, 2012) (top) and *Fxr* ChIP-Seq (Chong et al., 2010) (bottom) analysis of the *MafG* genomic loci showing locations of MafG exons and FXRE in the putative *MafG* proximal promoter functional in the liver. (J) Wild-type and FXRE mutant (mutated bases are bolded and underlined) MafG promoter (*MafG* prom) constructs upstream of a luciferase reporter gene were transfected into HepG2 cells with increasing amounts of a FXR expression plasmid and treated with vehicle or GSK2324 for 24 hours. Luciferase activity was normalized to β -galactosidase and expressed as fold change. All data shown as mean \pm SEM. Asterisks indicate statistically significant differences versus controls (** p<0.01; *** p<0.001). Different letters (a–d) indicate statistically significant differences (p<0.05).

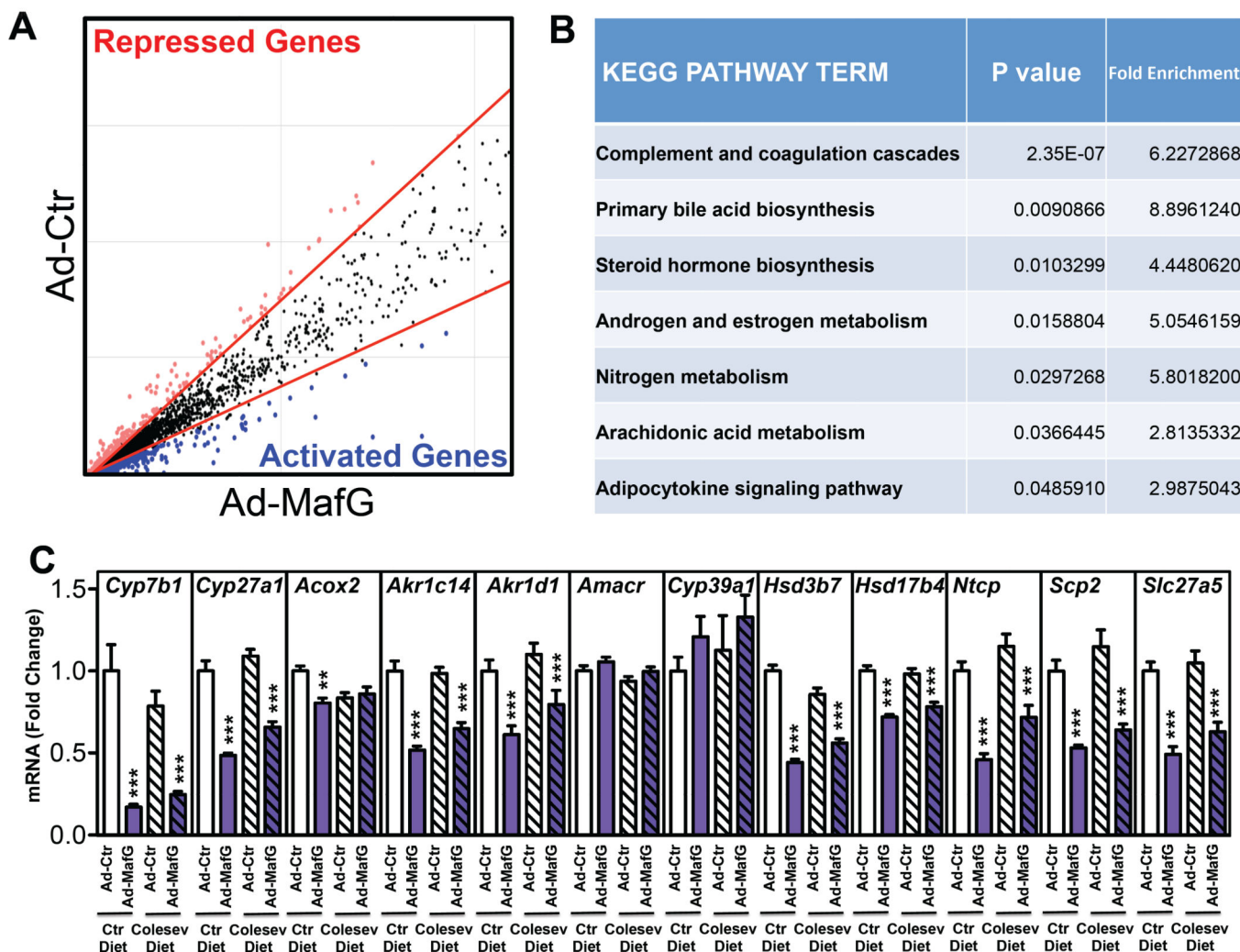


Figure 4. MAFG Regulates Several Genes Involved in Bile Acid Synthesis

(A) Microarray analysis of livers from mice treated with either Ad-control or Ad-MafG for 7 days. Lines delineate fold change cut-off (1.5-fold). Red and blue dots indicate genes that are repressed or induced genes, respectively ($n=3$ /condition). (B) KEGG pathway analysis for categories that were significantly enriched from global analysis of repressed genes in (A). (C) Hepatic expression of genes involved in bile acid synthesis or transport following treatment of C57BL/6 wild-type with Ad-control or Ad-MafG adenovirus for 7 days and fed either a control or Colesevelam-containing diet for 7 days prior and 7 days post adenovirus treatment ($n=8-9$ mice/group). All data shown as mean \pm SEM. Asterisks indicate statistically significant differences versus controls on the same diet (** $p<0.01$; *** $p<0.001$).

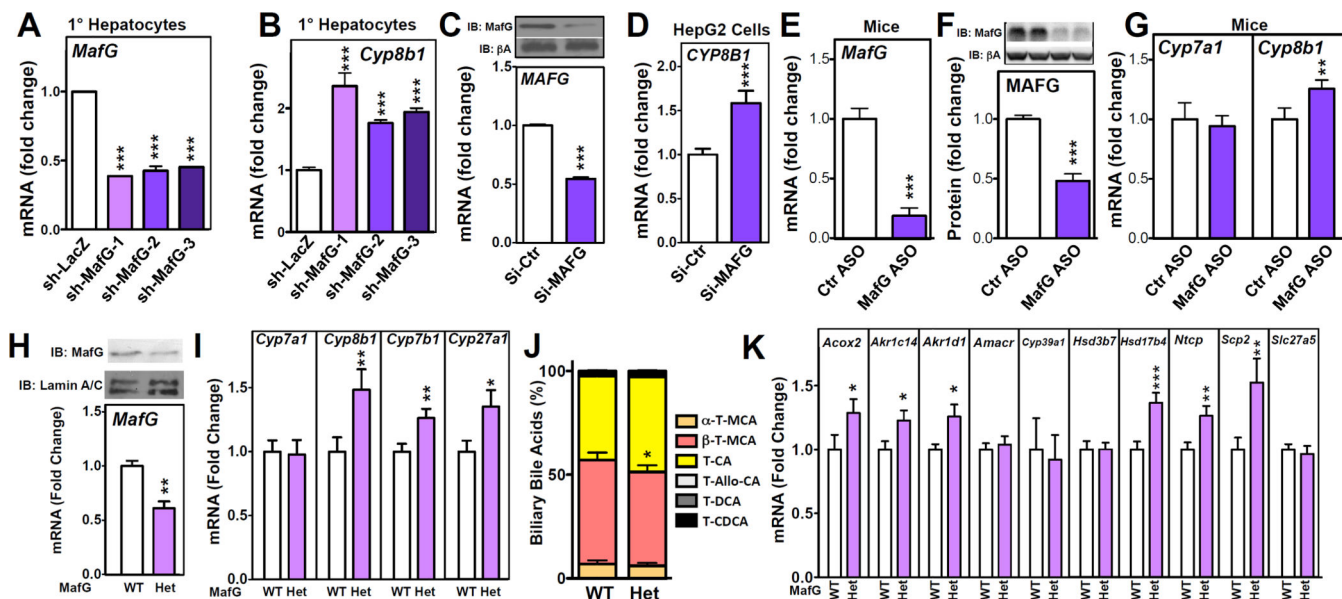


Figure 5. Loss of *MafG* Results in Derepression of Several Bile Acid Synthetic Genes

(A) Expression of *MafG* and (B) *Cyp8b1* in primary mouse hepatocytes treated with control (Ad-sh-LacZ), or three different *MafG* shRNA adenoviruses (Ad-sh-*MafG* 1–3) (n=4 wells/condition). (C) *MAFG* mRNA and protein (inset; pA, p-actin) and (D) *CYP8B1* expression in HepG2 cells treated with control or *MAFG* siRNA (n=3 wells/condition). (E–G) Hepatic *MafG* mRNA (E) and protein (F) *Cyp7a1* and *Cyp8b1* mRNA (G) in C57BL/6 wild-type mice treated with control or *MafG* ASO (100mpk) for 3 days (n=9 mice/group). (H) *MafG* mRNA and protein (top) and (I) *Cyp7a1*, *Cyp8b1*, *Cyp27a1* and *Cyp7b1* mRNA levels in littermate wild-type and *MafG*^{+/-} (Het) mice (n=7–11 mice/group). (J) Biliary bile acid levels were determined from individual littermate wild-type and *MafG*^{+/-} mice (n=7–11/group). (K) Hepatic expression of bile acid synthesis genes in littermate wild-type and *MafG*^{+/-} mice (n=7–11 mice/group). All data shown as mean ± SEM. Asterisks indicate statistically significant differences versus controls or wild-type (*p<0.05; **p<0.01; ***p<0.001).

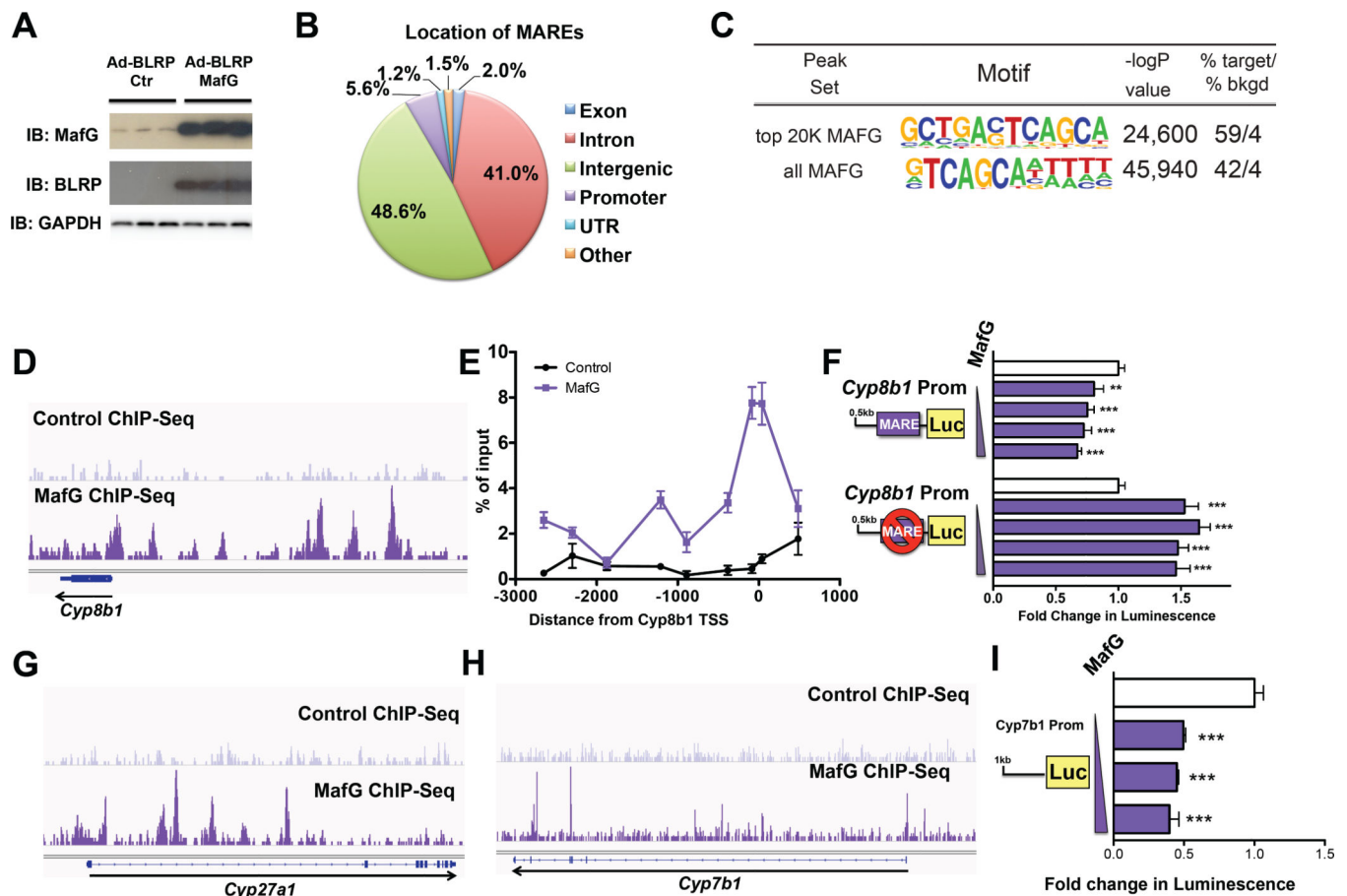


Figure 6. Identification of MAFG-Response Elements (MAREs) in Bile Acid Synthetic Genes

(A) Hepatic levels of MAFG protein levels (detected using anti-BLRP or anti-MAFG antibodies) in C57BL/6 mice treated with either control (Ad-BLRP) or BLRP-tagged MAFG adenovirus (Ad-BLRP-MafG). (B) Global frequency of hepatic MAFG binding sites (MAREs) across the genome relative to gene location (expressed as a percentage). (C) Table showing the motif for the top 20,000 peaks in MAFG ChIP-Seq peaks (top) and in all 68,754 peaks (bottom), with statistical significance and percent occurrence in peaks (target) or background (bkgd). (D) ChIP-Seq analysis of MAREs in chromatin isolated from livers of mice treated with Ad-BLRP (control; top) or Ad-BLRP-MafG (bottom) at *Cyp8b1* locus. (E) ChIP analysis of MafG occupancy at the *Cyp8b1* promoter region determined by RT-qPCR (primer locations to scale, Y axis). (F) Wild-type and MARE *Cyp8b1* promoter luciferase constructs were transfected into HepG2 cells and co-transfected with increasing amounts of a MAFG expression plasmid. Luciferase activity was normalized to p-galactosidase and expressed as fold change. (G–H) ChIP-Seq analysis of MAREs in chromatin isolated from livers of mice treated with Ad-BLRP (control; top) or Ad-BLRP-MafG (bottom) at loci for (G) *Cyp27a1* or (H) *Cyp7b1*. (I) *Cyp7b1* promoter-luciferase reporter transfected into HepG2 cells together with increasing amounts of a MAFG expression plasmid. Luciferase activity was normalized to p-galactosidase and expressed as fold change. All data shown as mean \pm SEM. Asterisks indicate statistically significant differences from control (** $p < 0.01$; *** $p < 0.001$).

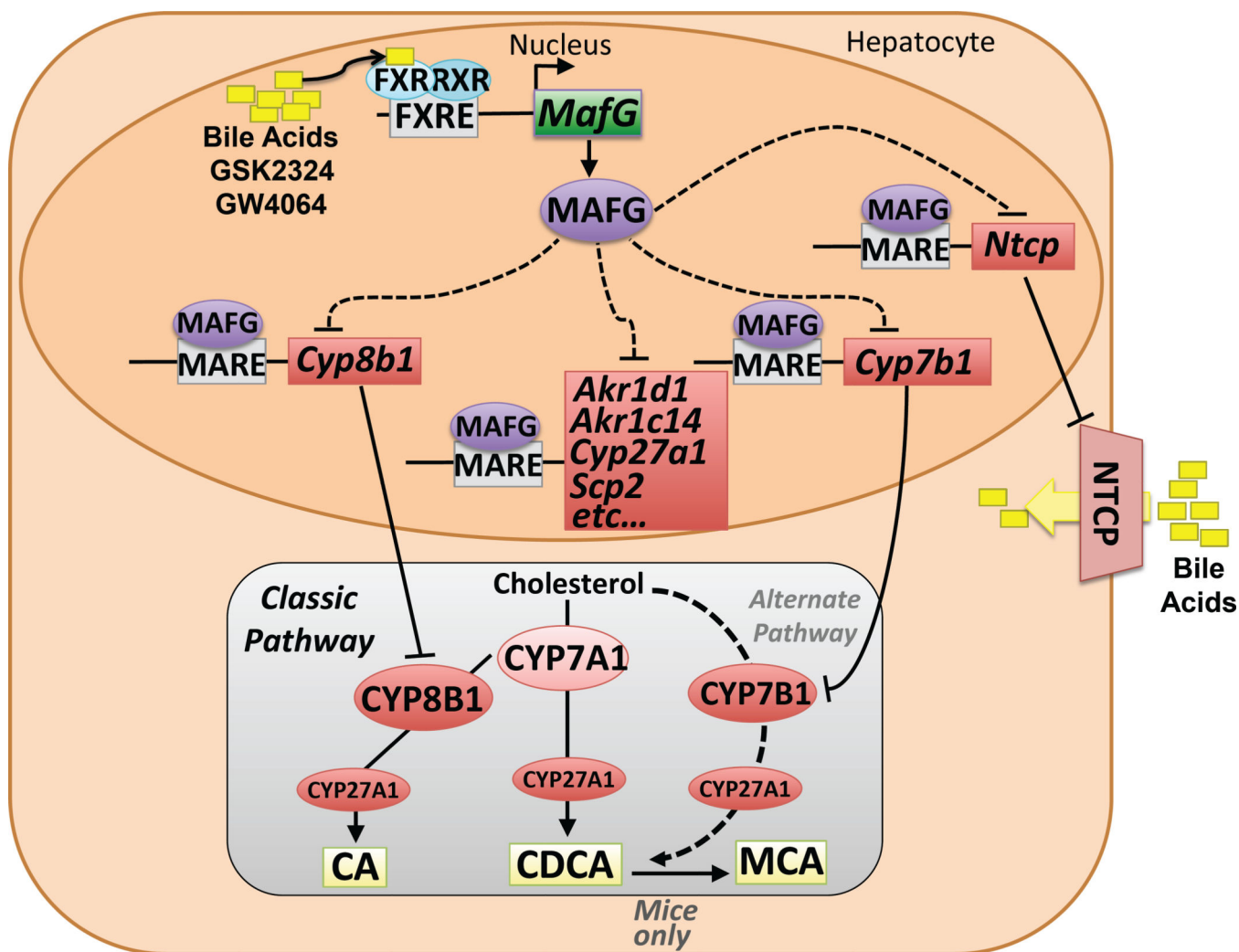


Figure 7. Summary for the Role of MAFG in Regulating Bile Acid Synthesis and Transport
 The cartoon shows the activation of the *MafG* gene following FXR activation by various ligands (yellow boxes), and the subsequent targeting of MAFG protein (purple) to several MAREs. MAREs identified in the current study that lie within the genomic loci of MAFG-repressed genes (shown in red) that encode proteins involved in bile acid synthesis or metabolism are identified. Below is a simplified version of the classic and alternative bile acid synthetic pathways that generate cholic acid (CA), chenodeoxycholic acid (CDCA) or muricholic acid (MCA).